

Controlled Encapsulation and Release of Substances based on Temperature- and Photo-responsive Nanocapsules

Xiaotao Wang^a, Tong Huang^a, Wing-Cheung Law^{b}, Ching-Hsiang Cheng^{b*}, Chak-Yin Tang^b, Ling Chen^b, Xinghou Gong^a, Zuifang Liu^a, Shijun Long^a*

a. Hubei Provincial Key Laboratory of Green Materials for Light Industry, Collaborative Innovation Center for Green Light-weight Materials and Processing, School of Materials Science and Engineering, Hubei University of Technology, Wuhan, Hubei Province 430068, P.R. China.

b. Department of Industrial and Systems Engineering, The Hong Kong Polytechnic University, Hung Hom, Kowloon, Hong Kong SAR, P.R. China

*Corresponding author roy.law@polyu.edu.hk, ching-hsiang.cheng@polyu.edu.hk

Abstract

In this study, dual-responsive polymeric nanocapsules, in which the state (swelling or collapse) can be repeatedly controlled by external stimuli (i.e., temperature and light), have been designed and prepared through distillation-precipitation polymerization. Temperature sensitive monomers of N-isopropylacrylamide are crosslinked by photoresponsive bis (methacryloylamino) onto a silica nano-spherical template to form a core-shell (SiO₂-PNIPAM/Azo) structure. The silica core is then removed by hydrofluoric acid to produce PNIPAM/Azo nanocapsules (P/ANCs) of diameter ~238 nm at ~25°C. The size of the nanocapsule is temperature responsive and, as such, its

diameter could be reduced to ~182 nm on increasing the temperature to 40°C. In addition, the permeability of nanocapsules can be adjusted by UV irradiation. The *cis-trans* transformation of modified azobenzene allowed us to perform both the encapsulation and controlled release of molecules. Rhodamine B (RhB) was successfully encapsulated using the photomechanical method. In controlled release experiments, after the majority of RhB (~45%) was released from the P/ANCs using temperature (~40°C) and UV light, a second stage of release could be triggered by lowering the temperature (~18.4%) and applying UV-Visible lighting cycles (~29.4%), respectively. We found that the diffusion coefficient, *D*, was 45% larger under alternate irradiation than UV light alone. Our results demonstrate considerable potential for customizable delivery systems for a variety of drugs.

Introduction

There are various methods for preparing drug-containing nanomaterials to enhance the precision and efficacy of a drug in treating diseases ¹. The remote-controlled release of therapeutics has also received an increasing amount of attention, a method that could address the same issues ². Intelligent drug delivery systems could control dosage for patients' specific needs ³. Furthermore, systems could prevent undesirable side effects on normal tissue by minimising the release of medicine before arriving at the infected sites ^{4,5}. Indeed, how to achieve a uniform, stable encapsulation and controlled release within a single system is a question of great concern for drug delivery systems.

Light, magnetic fields, electric fields and heat have been used as the main external physical stimuli to trigger the release of therapeutics ⁶⁻⁹. Light stimulation can provide

more flexibility and control for personalised treatment, due to its remote control and rapid switchable capabilities ¹⁰. Azobenzene chromophores have been extensively investigated in recent years because of their excellent reversible photo isomerization properties and easily functionalised structures ¹¹. They can be transformed from their hydrophobic trans- form to relatively hydrophilic cis-isomers when the distance between the 4- and 4'-carbons changes from 9.0 Å to 5.5 Å and the corresponding dipole moment changes from 0 D to 3 D ^{12,13}. Typically, photoresponsive vesicles are always prepared by self-assembly with azobenzene block copolymers because of the inhibition polymerization of the azo groups. Zhao and Wang used amphiphilic copolymers containing azo groups to self-assemble colloidal aggregates. By interchanging UV and visible light irradiations, the self-assembly aggregates undergo reversible dissociation and reorganization ¹⁴⁻¹⁷. Similarly, Zhang and co-workers successfully harnessed the self-assembly and disassembly properties of a hydrophilic block ionomer and azo-containing surfactant to construct light-controlled microcapsules that were capable of assimilating and releasing objective molecules ¹⁸. In another study, Bédard used a layer-by-layer self-assembly method to prepare microcapsules containing azobenzene moieties. Light-controlled release through the photo-induced disassembly of the microcapsules was achieved ¹⁹. Moreover, the light-controlled release rate was found to depend on the disassembly rate of azobenzene-containing macromolecules ²⁰. If the azobenzene content is too low, the disassembly process of photoresponsive micelles caused by variation in the dipole moment under UV irradiation may be ineffective. Yu reported NIPAM and azobenzene block copolymer micelles with dual responsive

properties ²¹. However, the UV irradiation could not disrupt the micelles without releasing the encapsulated substances.

There is little research on the photo-controlled, stable encapsulation of drugs. Sukhorukov and his colleagues studied the optically driven encapsulation of microcapsules constructed by photosensitive moieties ^{22, 23}. First, they reported micron-sized capsules constructed of poly (diallyldimethyl ammonium chloride) (PDADMAC) and poly (styrene sulfonate) (PSS). They demonstrated that heat was capable of shrinking the capsules' shells, which made them impermeable to other substances and thus suitable for stable encapsulation. They then fabricated poly (methacrylic acid)-poly (allylamine hydrochloride) microcapsules modified with UV-responsive benzophenone groups using the layer-by-layer technique. They found a 30% shrinkage on the capsules after 2 hours of 275 nm irradiation. The photo-induced variation of shell permeability thus enables stable encapsulation without leakage, which is a useful feature for targeted drug delivery.

Our group has devoted considerable efforts to synthesising robust photo-responsive microcapsules ^{24, 25}. In the present research, a novel distillation-precipitation-polymerization approach is presented for fabricating multi-responsive capsules at the nanometer scale. In this approach, the incorporation of photo-responsive bis (methacryloylamino)-azobenzene (BMAAB) as the cross-linker is an important step. The dual role of BMAAB allows us to adjust the permeability of the nanocapsules with the aims of stabilising the encapsulation, avoiding undesired leakage and, ultimately, controlling the release of the drug upon exposure to UV irradiation. Furthermore, poly

(N-isopropylacrylamide) (PNIPAM) was used as the temperature responsive polymer²⁶⁻²⁹ and the basic material of our nanocapsules as a way to confer dual-responsiveness. This study shows that the use of light for nanomechanical control is highly promising for encapsulating and discharging Rhodamine B (RhB).

Experimental Section

Materials

Chemical Reagent Co., Ltd, Jiangsu, China, supplied methacrylic acid, 1-Ethyl-3-(3-dimethylaminopropyl) carbodimide hydrochloride (EDC·HCl), and HCl (1N), while 3-Methacryloxypropyltrimethoxysilane (MPS) was purchased from the Organic Silicon Company at Wuhan University, China. Technical grade divinylbenzene (DVB, 45% concentration, Sinopharm Group Chemical Reagent Co., Ltd, Shanghai, China) was washed with a 5% aqueous solution of sodium hydroxide in water and later dried over anhydrous magnesium sulphate. High-purity azobisisobutyronitrile (AIBN) was recrystallised by ethanol. Acetonitrile (Sinopharm Group Chemical Reagent Co., Ltd, Shanghai, China) was dried over calcium hydride and purified by distillation prior to use. Distilled tetrahydrofuran (THF, spectroscopic grade) was run through 4 Å molecular sieves to remove water traces. Hydrofluoric acid (HF, containing 40% of HF) and analytical grade N-isopropylacrylamide were supplied by Tianjin Chemical Reagent Factory and Damao Chemical Reagent Factory, Tianjin, respectively. Sinopharm Group Chemical Reagent Co., Ltd, Shanghai, China, supplied the other chemicals, which were used in their as-received state.

Synthesis of BMAABbis(methacryloylamino)-azobenzene

4, 4'-diaminoazobenzene (DAAB) was synthesised based on 18. BMAAB was

prepared by using a mild dehydration reaction³⁰. In a typical experiment, 800 mL of chloroform was used to dissolve 2 g of DAAB contained in a flask. Subsequently, methacrylic acid (10 mL) and EDC·HCl (3.61 g) were each added to the flask and stored at ambient temperature for three days. The resulting organic solution was washed with water and dried over magnesium sulphate. Furthermore, the solution was subjected to a low-pressure evaporation and later recrystallized with ethanol. Finally, BMAAB was obtained by drying the crystals at 50°C.

Synthesis of silica nanospheres with NIPAM shell crosslinked by Azo (SiO₂-PNIPAM/Azo)

Vinylated silica nanospheres were synthesised based on 20. Distillation precipitation polymerization was used to prepare PNIPAM/Azo@SiO₂ nanospheres. In this protocol, vinylated SiO₂ particles, thermal-responsive NIPAM, BMAAB, and DVB were used as template, monomer, cross-linker and assistant cross-linker, respectively. Typically, 0.2 g of vinylated silica particles was placed in a 250 mL flask with 160 mL of acetonitrile and ultra-sonicated for half an hour, before BMAAB (0.7452 g), NIPAM (1.1316 g), DVB (42 µL) and AIBN (0.0226 g, 2 wt% with reference to the comonomer) were added into the flask. The flask was fitted with a condenser, an oil-water extractor, a receiver, and a nitrogen protection device. The whole reaction equipment was heated to 80°C over 30 min, and kept for 15 min, before being raised to 100°C. Eighty millilitres of acetonitrile was distilled within 4.5 hours (including the heating time). After the reaction ended, a small amount of hydroquinone, acting as a polymerization inhibitor, was added to the flask and continuously stirred until the content of the flask

reached ambient temperature. A yellow solid was collected, centrifuged three times for purification, and re-dispersed in ethanol or THF. Finally, the resultant SiO₂-PNIPAM/Azo core-shell nanospheres were vacuum-dried.

Synthesis of PNIPAM/Azo nanocapsules (P/ANCs)

P/ANCs were prepared by using HF acid to selectively etch the SiO₂ core. The dried SiO₂-PNIPAM/Azo nanospheres were immersed in excess HF acid for 24 hours. The purified product was obtained over several centrifugation cycles and re-dispersed in ethanol (clear solution).

Loading and release of Rhodamine B

A mixture of 20 mL of RhB solution (1.5 mg/mL) in ethanol and PNIPAM/Azo nanocapsules (40 mg) was magnetically stirred for 24 hours at ambient temperature. The resultant solution was then subjected to centrifugation at 10000 rpm, and the resultant precipitation was washed with ethanol until it was completely free of RhB on the nanospheres' surface. The whole washing process was completed in 15 min. The loading capacity of the RhB molecules was measured using fluorescence spectroscopy at a wavelength of 565 nm with an excitation wavelength of 420 nm. The RhB-loaded PNIPAM/Azo nanocapsules were gained as a powder.

Thermal-responsive release behavior of the P/ANCs

A total of 10 mg of RhB-loaded PNIPAM/Azo nanocapsules were added to 5 mL of water and contained in a dialysis bag that had a 8,000-10,000 kDa molecule-weight cut-off. The dialysis bag was placed in a container with 13 mL of ethanol and maintained at 40°C in a water bath. Periodically, about 4 mL of the solution was withdrawn from

the container for fluorescent spectroscopic analysis to assess the concentration of RhB discharged in the solution. The analysis was conducted at an excitation wavelength of 480 nm before the test solution was returned to its container.

Photo-responsive release behavior of the P/ANCs

The procedure followed was the same as that described in the previous section. Two additional samples were also prepared. Each of these three containers was irradiated with UV, visible light, and alternating UV/visible light. Periodically, about 4 mL of solution was withdrawn from the container for fluorescent spectroscopic analysis to assess the concentration of RhB discharged in the solution. The analysis was conducted at an excitation wavelength of 480 nm before the test solution was returned to its container.

Characterizations

A Bruker Equinox 55 Fourier spectrometer was used to record the Fourier transform infrared (FTIR) spectra using a KBr disc. Electron microscopy images were obtained using a Tecnai G 220 (PEI Co.) transmission electron microscopy (TEM). An FP-6500 fluorescence spectrometer was used to analyse the fluorescence spectra of the samples. Dynamic laser scattering (DLS) measurements were performed on a Brookhaven 90Plus laser light scattering spectrometer at a scattering angle of 90°. Photo-isomerization experiments were carried out using 365 nm of light from an ultraviolet lamp (16 W, zf-7A, Shanghai Gucun Electron Optic Instrument Factory), with an intensity of $\sim 1.5 \text{ mW/cm}^2$. The volume of the solution was $\sim 4 \text{ mL}$ and the duration was 10 min for the trans-isomers to be transformed to cis-isomers.

Particle Size Analysis

A Philips-XL-30 scanning electron microscopy (SEM) was used to image about 100 particles and estimate their polydispersity index (U), using the following formula ³¹:

$$U = D_w / D_n$$
$$D_n = \sum_{i=1}^k n_i D_i / \sum_{i=1}^k n_i$$
$$D_w = \sum_{i=1}^k n_i D_i^4 / \sum_{i=1}^k n_i D_i^3$$
(1)

where D_n , D_w , n and D_i are the number-averaged diameter, weight-averaged diameter, total number of measured particles and diameter of the nanospheres, respectively.

3 Results and discussion

Morphology of P/ANCs

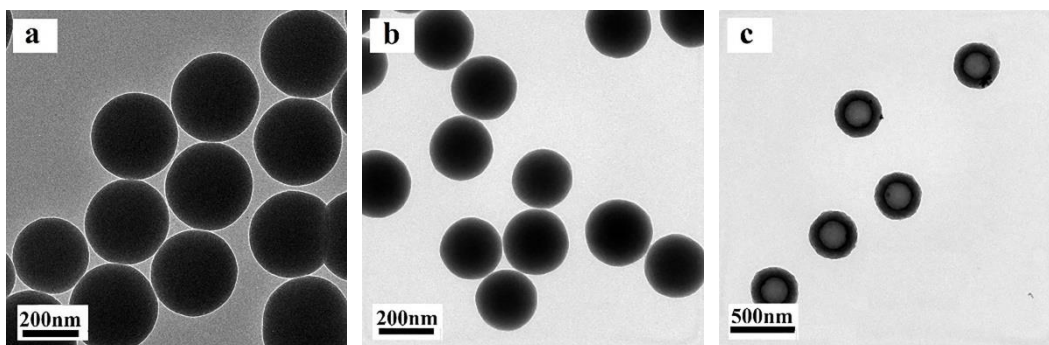


Fig. 1 TEM images of (a) silica particles, (b) SiO₂-PNIPAM/Azo and (c) P/ANCs.

In the distillation precipitation polymerization of SiO₂-PNIPAM/Azo nanospheres, silica nanoparticles, thermal responsive NIPAM and photoresponsive BMAAB were used as the template, monomer and cross-linker, respectively. The dual role of BMAAB, which acted as both a photo-responsive element and a cross-linker, is an important component in precipitation polymerization. As shown in Fig. 1(a), the monodisperse silica nanoparticles of diameter ~250 nm, prepared via the Stöber method, were

obtained. The successful formation of a uniform silica-PNIPAM/Azo core-shell structure (SiO_2 -PNIPAM/Azo) can be clearly observed in Fig. 1(b). The average particle size increased to ~ 430 nm after the deposition of the PNIPAM/Azo shell. The silica core was subsequently etched by HF to yield P/ANCs with a shell thickness of 90 nm (Fig. 1(c)). The polydispersity index was estimated to be 1.01 according to Equation (1), indicating a high monodispersity of the nanoparticles. The supporting information in Fig. S1 shows the infrared spectra of the vinylated silica particles, SiO_2 -PNIPAM/Azo nanospheres and PNIPAM/Azo nanocapsules, providing further proof of their structure.

Thermal responsive behavior of P/ANCs and controlled release

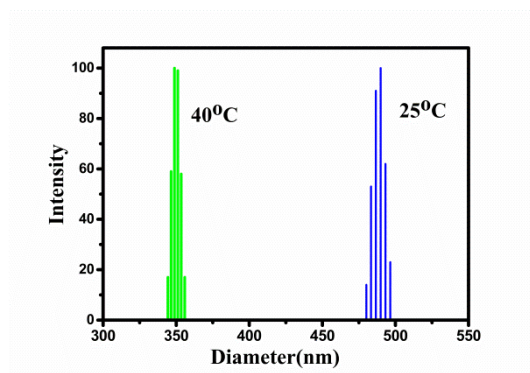


Fig. 2 Hydrodynamic diameters (D_h) of P/ANCs and their size distribution in aqueous solution at (a) 40°C (Green) and (b) 25°C (Blue).

Fig. 2 shows the variation in the hydrodynamic diameters (D_h) of P/ANCs, which increased from ~ 350 nm to ~ 489 nm when the temperature decreased from 40°C to 25°C. This suggests that the collapsed structure of increased-size nanocapsules would induce further release with temperature shifts. The D_h of P/ANCs decreased from ~ 489 nm at room temperature to ~ 350 nm at 40°C, which can be attributed to the shrinkage

of the PNIPAM/Azo shell. The hydrophilic amide groups and hydrophobic isopropyl parts in the PNIPAM molecules contribute to the structural transformation under different temperatures. When the temperature is lower than critical solution temperature (LCST), the interaction between the hydrogen bonds and the amide groups of PNIPAM can make the water molecules around the macromolecule chains form a higher degree of ordering solvation layer and extend the macromolecules structure. With an increase in temperature, the hydrogen bonds between the amide groups and water are disrupted, and water molecules, being a poor solvent, begin to be expelled from the PNIPAM/Azo layer, thereby leading to a collapsed structure.

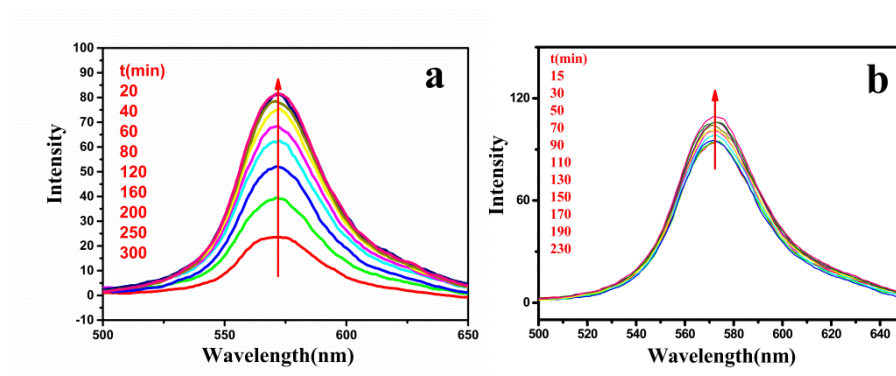


Fig. 3 Fluorescence spectra of the RhB (a) release from P/ANCs at 40° C and (b) during the process of cooling to room temperature(25° C)

After RhB was successfully loaded in the microcapsules, the release behavior was investigated by measuring the fluorescence intensities. Fig. 3(a) shows the fluorescence spectra of RhB released from P/ANCs at 40°C, while Fig. 3(b) shows the process of cooling to room temperature (25°C). As time increased, the intensity of the RhB molecules released from P/ANCs at 565 nm also increased, attaining equilibrium after 180 min at 40°C, corresponding to 48.5% of the RhB molecules. This is due to the

temperature (40°C) being above the 32°C LCST of PNIPAM and the hydrophobic layer hindering the movement of the polymer chains, which decreases the shell permeability. After the release equilibrium was reached, the nanocapsules were allowed to cool down to room temperature. Fig. 3(b) shows the change in fluorescence intensity during this period. Clearly, additional RhB molecules (~18.4%) were released from P/ANCs due to the change in temperature. When the temperature was decreased slowly to LCST, the polymer chains on the shell started stretching out. When the hydrodynamic diameters (D_h) of the P/ANCs were increased from ~350 nm to ~489 nm by decreasing the temperature from 40°C to 25°C, the collapsed structure of the nanocapsules with increased permeability induced further large releases (~18.4%) from the P/ANCs.

This result corroborates the findings of other studies, which report similar temperature-controlled releases with large variations in microcapsule size inducing different release rates at different temperature. Yang reported on the properties of double-walled PNIPAM-PMMA microcapsules with dual stimuli-responsive properties and suggested that their low release rate was due to the shrinkage of the PNIPAM and PMMA cross-linked shells, which serve as the outer and inner layers, respectively ³². As the solution temperature decreased, the outer PNIPAM shell became swollen and resulted in a further (~20%) release of the drug from the hollow nanospheres. Liu prepared pH/ionic strength/temperature multi-responsive microcapsules, achieving a temperature-responsive controlled release ³³. Chaudhary reported a facile synthesis of pH- and temperature-responsive poly (N-isopropylacrylamide) nanogels, similarly suggesting potential for controlled-temperature drug release. Wang Guojie designed

novel multi-stimuli-responsive nanogels, similarly demonstrating the possibility of release triggered by temperature, pH and UV light. In our work, the P/ANCs exhibited mutually independent responsive behavior triggered by temperature and light.

Photo-responsive behaviors of P/ANCs and controlled release

The UV-vis spectra in Fig. S2 were used to study the photo-responsive behavior of P/ANCs. The photo-stability of P/ANCs was recorded after 10 min and their recovery to the trans-structure was completed in 30 min. Obviously, the reversible photo-isomerization behavior of P/ANCs are smoothly realised when exposed to UV and visible light irradiation. On the transformation of the trans-isomer to cis-isomer, a decreased distance of cross-linking sites appeared to be due to the size variation of the different structures. This leads to the movement of the whole shell, as depicted in Scheme 1. The structure of the shell is restored under exposure to visible light due to the reversible photo-isomerization behavior. To certify the effects of photo-isomerization behaviors on the shell, the diameters of P/ANCs before and after 30 min irradiation of UV light were investigated through DLS, as shown in Fig. 4. The hydrodynamic diameter (D_h) of the P/ANCs decreases from 489 nm to 368 nm upon UV irradiation.

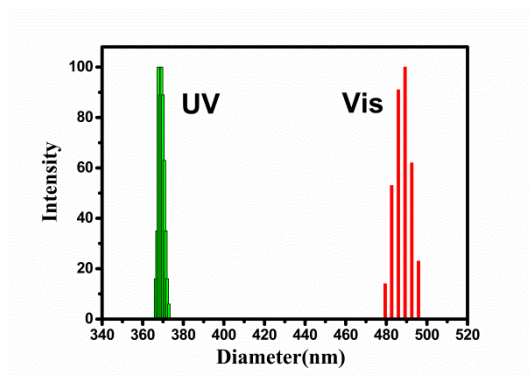
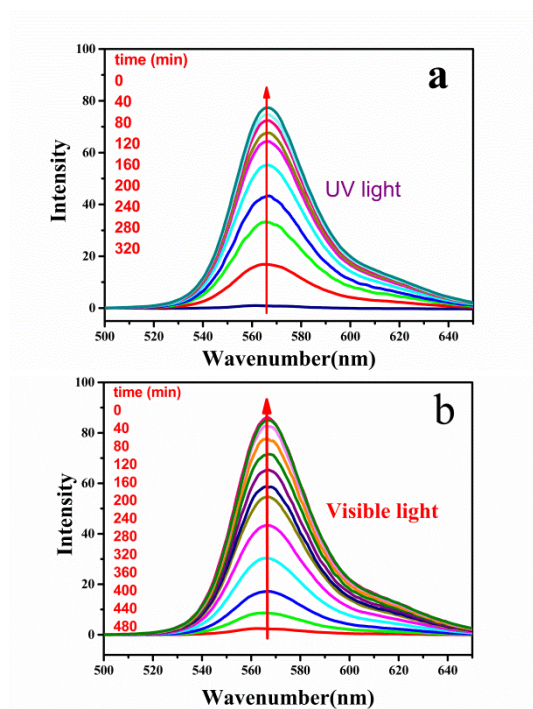


Fig. 4 Diameters of P/ANCs before and after 30 min irradiation of UV light.

Similar photo-induced shrinkage behaviors, arising from the transformation of azobenzene moieties, have been reported in the literature and are known to be photomechanical effects³⁴⁻³⁷. Baczowski et. al. realised photomechanical effects in azobenzene-functionalised polyimides, showing large deformations³⁴. Similarly, Kulawardana synthesised photo-responsive oil sorber (POS) from monomers of 4-(methacrylamino) azobenzene, cross-linked with bis (methacryloylamino) azobenzene. The POS provided a photo-responsive shell surrounding a hydrophobic core. The absorption and desorption properties of POS could be controlled by the irradiation of UV light³⁸.

Fig. S2 shows that a time of 10 min is required to attain an equilibrium state for cis-isomers under UV irradiation, while a reversal to the trans-isomer state under the influence of visible light takes 30 min. In a cycle of alternating light irradiation, the respective durations for UV and visible light are 10 and 30 min.



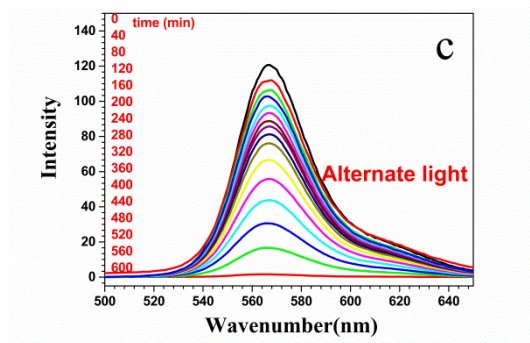


Fig. 5 Fluorescence spectra of RhB release from the P/ANCs under (a) UV irradiation, (b) visible, and (c) UV-Vis cycles.

Fig. S3 shows the fluorescence microscopy images of (a) PNIPAM/Azo nanocapsules loaded with RhB, (b) after 24 hours with the PNIPAM/Azo nanocapsules (c) when the solution is taken out of the dialysis bags, and indicates that RhB was successfully encapsulated and released by diffusion.

The cumulative release profile of RhB from the P/ANCs under UV irradiation, visible light and the UV-Vis cycles is shown in Fig. 5. It can be clearly seen that the emission peak at 565 nm increases with time until reaching equilibrium. It is important to note that the released quantities at the equilibrium are different, and the cumulative release is maximum under UV-Vis alternate irradiation cycles, while the minimum release is found in UV irradiation.

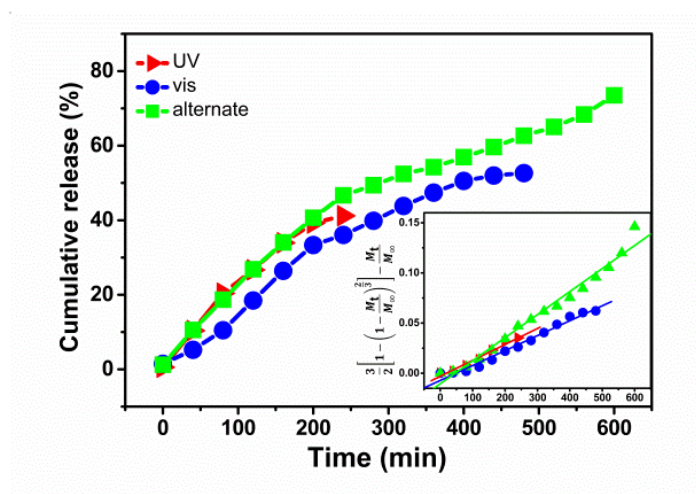


Fig. 6 Release of RhB from P/ANCs as a function of time (setting the largest release quantity as 100%), under

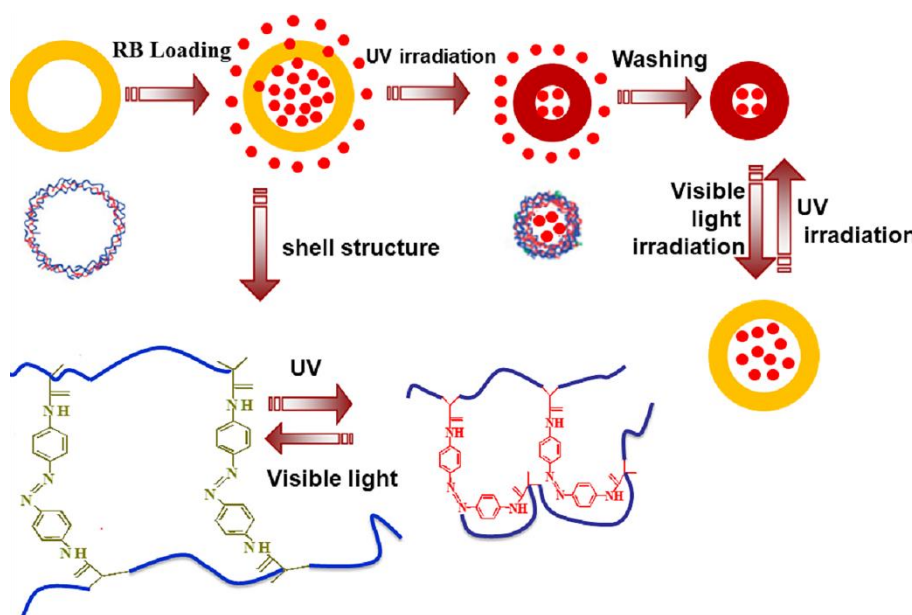
alternate light (1), visible light (2) and UV irradiations (3)

Initially, the release rate under UV irradiation was rapid and attained equilibrium after 320 min with 44.1% of cumulative release. The shrinkage of the structure led to the extrusion of encapsulated molecules out of the shell, which explains the fast release rate at the initial state. Similar observations – that this kind of extrusion effect is due to shrinkage – can be found in the literature. For instance, Chen et al. prepared Fe₃O₄/PNIPAM nanospheres and found that the shrinkage of the shell led to the release of drug molecules with an increase in temperature³⁹. Other research suggested that the shrinkage-induced compact structure might be used as a drug carrier for stable encapsulation⁴⁰.

In our work, with trans-azobenzene transformed to cis-structure at the junction, the shrinkage of the shell network triggered the release of RhB from the core at a very fast initial rate. However, after shrinkage, the increase in shell density caused a decrease in permeability and hence a decrease in the release rate. The total release level became stable at 44.1% in 320 min (Fig. 6, red curve). As for visible light irradiation, an additional 8.6% of RhB molecules was released to reach 52.7%, as shown in Fig. 6 (blue curve). Interestingly, when we repeated the UV-Vis irradiation cycles, the accumulation of RhB was eventually “squeezed out” (Fig. 6, green curve).

Under alternating UV/visible light irradiations, two processes are likely to be involved. The first UV irradiation process causes the shrinkage of P/ANCs and squeezes the RhB from the hollow core. On irradiation with visible light, azobenzene at the junction reverts to its trans-isomer state, causing the shell to expand to its original state. The decreased density and increased permeability of the shell during reversion

both favour the release of RhB. Under alternate light irradiation cycles, as shown in Scheme 1, the cumulative release of RhB reached 73.5% at 600 min. By adjusting the frequency of the UV-Vis cycle, it may be possible to control the release rate using a “pulsed” signal. This photo-mechanical effect was also shown in azobenzene-modified mesoporous silica systems, in which the continuous photo-isomerization azobenzene groups in the mesopores of silica acted as “stirrer” to achieve the desired release.



Scheme 1. Schematic diagram of the photomechanical loading of RhB and the release process using the UV-Vis cycle

Various models describe the release of drugs from different matrices. The Baker–Lonsdale model is widely used for modelling the controlled release of drugs from a spherical matrix⁴¹⁻⁴⁵.

$$\frac{3}{2} \left[1 - \left(1 - \frac{M_t}{M_\infty} \right)^{\frac{2}{3}} \right] - \frac{M_t}{M_\infty} = \frac{3DC_s}{r_0^2 C_0} \cdot t \quad (2)$$

where M_t and M_∞ are the amounts of target molecules at time t and at infinite time, respectively; the ratio of M_t/M_∞ is the cumulative release of target molecules; D is the diffusion coefficient of the molecules from the matrix; r_0 is the radius of the

nanocapsule; C_s is the solubility of the target molecule in the matrix and C_0 is the original concentration of the target molecule. The results in Fig. 6 show that the Baker–Lonsdale model is a good fit for the release profile of RhB under different illuminations. Therefore, the release rate constants ($3DC_s/r_0^2C_0$) and the correlation coefficients R^2 are $1.58 \times 10^{-4} \text{ min}^{-1}$ and 0.99 under UV, $1.49 \times 10^{-4} \text{ min}^{-1}$ and 0.98 under visible light, and $2.29 \times 10^{-4} \text{ min}^{-1}$ and 0.99 under alternate irradiation, respectively. Assuming that C_s and C_0 can be considered equivalent in a steady release system, the diffusion factor D under alternate irradiation is 45% larger than under UV. The accelerated release behavior, as observed in the shrinking-swelling cycles, demonstrates the realization of photo-mechanically driven release. As such, our work demonstrates the promising approach of using photomechanical phenomena to achieve encapsulation and discharge of particles from nanocapsules.

Conclusions

Distillation precipitation polymerization was used to synthesise nanocapsules with a shell layer of c. 90 nm. The nanocapsules exhibited excellent photo- and thermal-induced responses. TEM and SEM images showed that they were monodispersed and had a robust hollow structure. The UV-induced transformation of azobenzene group from trans- to cis-isomers resulted in denser shells and influenced their encapsulation and release behaviors. Under UV irradiation, the permeability of nanocapsules could be adjusted, thus permitting a novel molecular encapsulation method for hollow cores. By using alternate light irradiation, maximal control of the release was achieved, owing

to frequent changes in the shell networks as the transformation between trans- and cis-isomers was repeated. This photomechanical effect was further demonstrated by the azobenzene moiety tethered on the surface of the amorphous silica system. This approach is expected to have important applications in the development of encapsulation and release systems controlled by photo stimuli and temperature-sensitive materials and membranes.

Supporting Information Available

FT-IR spectra curves of silica particles with the vinyl group, SiO₂-PNIPAM/Azo nanospheres and P/ANCs. UV-vis spectra at 365 nm of 0.1 mg/mL of P/ANCs dissolved in ethanol under UV irradiation (a) and after being kept in the dark at 23 °C (b). In addition, fluorescence microscopy images of RhB-loaded P/ANCs, after the release of RhB for 24 h and the solution outside the dialysis tube.

Acknowledgements

This work was supported by the Research Committee of The Hong Kong Polytechnic University (G-UA4G and G-YBMY) and the Natural National Science Foundation of China (51303049, 61405169 and 51603065). Hubei province natural science foundation of China 2014CFB603.

References

- (1) Qin, H. J.; Cui, B.; Li, G. M.; Yang, J. H.; Peng, H. X.; Wang, Y. S.; Li N. N.; Gao, R. C.; Chang, Z. G.; Wang, Y. Novel Fe₃O₄@ZnO@mSiO₂ Nanocarrier for Targeted Drug Delivery and Controllable Release with Microwave Irradiation. *J. Phys. Chem. C*, **2014**, 118, 14929–14937
- (2) Singh, A.; Talekar, M.; Tran, T.; Samanta, A.; Sundaram, R.; Amiji, M. Combinatorial Approach in the Design of Multifunctional Polymeric Nano-delivery Systems for Cancer Therapy. *J. Mater. Chem. B*, **2014**, 2, 8069–8084.
- (3) Zhang, J.; Fu, Y.; Jiang, F.; Lakowicz, J. R. Magnetically Sensitive Alginate-templated Polyelectrolyte Multilayer Microcapsules for Controlled Release of Doxorubicin. *J. Phys. Chem. C*, **2010**, 114, 7673–7679

- (4) Igarashi, E. Factors Affecting Toxicity and Efficacy of Polymeric Nanomedicines. *Toxicol. Appl. Pharmacol.*, **2008**, 229, 121–134.
- (5) Malam, Y.; Loizidou, M.; Seifalian, A. M. Liposomes and Nanoparticles: Nanosized Vehicles for Drug Delivery in Cancer. *Trends Pharmacol. Sci*, **2009**, 30, 592–599.
- (6) Li, C.; Luo, G. F.; Wang, H. Y.; Zhang, J.; Gong, Y. H.; Chuo, R. X.; Zhang, X. Z. Host–guest Assembly of pH-responsive Degradable Microcapsules with Controlled Drug Release Behavior. *J. Phys. Chem. C*, **2011**, 115, 17651–17659
- (7) Guo, H. X.; Zhao, X. P.; Guo, H. L.; Zhao, Q. Preparation of Porous SiO₂/Ni/TiO₂ Multicoated Microspheres Responsive to Electric and Magnetic Fields. *Langmuir*, **2003**, 19, 9799–9803.
- (8) Ge, J.; Neofytou, E.; Cahill, T. J.; Beygui, R. E.; Zare, R. N. Drug Release from Electric-field-responsive Nanoparticles. *ACS Nano*, **2012**, 6, 227–233.
- (9) Urbina, M. C.; Zinoveva, S.; Toby, M.; Sabliov, C. M.; Monroe W, T.; Kumar, C. S. S. R. Investigation of Magnetic Nanoparticle–polymer Composites for Multiple-controlled Drug Delivery. *J. Phys. Chem. C*, **2008**, 112, 11102–11108.
- (10) Bédard, M. F.; Geest, B. G. D.; Skirtach, A. G.; Möhwald, H.; Sukhorukov, G. Polymeric Microcapsules with Light Responsive Properties for Encapsulation and Release. *Adv. Colloid Interf*, **2010**, 158, 2–14.
- (11) Samai, S.; Bradley, D. J.; Choi, T. L. Y.; Yan, Y.; Ginger D. S. Temperature-Dependent Photoisomerization Quantum Yields for Azobenzene-Modified DNA. *J. Phys. Chem. C*, **2017**, 121, 6997–7004.

- (12)Finkelmann, H.; Nishikawa, E.; Pereira, G. G.; Warner, M. A New Opto-mechanical Effect in Solids. *Phys. Rev. Lett.*, **2001**, 87, 015501.
- (13)Jiang, J. Q.; Tong, X.; Morris, D.; Zhao, Y. Toward Photocontrolled Release using Light-dissociable Block Copolymer Micelles. *Macromolecules*, **2006**, 39, 4633–4640.
- (14)Ikeda, T.; Nakano, M.; Yu, Y. L.; Tsutsumi, O.; Kanazawa, A. Anisotropic Bending and Unbending Behavior of Azobenzene Liquid-crystalline Gels by Light Exposure. *Adv Mater*, **2003**, 15, 201–205.
- (15)Tong, X.; Wang, G.; Soldera, A.; Zhao, Y. How can Azobenzene Block Copolymer Vesicles be Dissociated and Reformed by Light? *J Phys Chem B*, **2005**, 109, 20281–20287.
- (16)Li, Y. B.; Deng, Y. H.; Tong, X. L.; Wang, X. G. Formation of Photoresponsive Uniform Colloidal Spheres from an Amphiphilic Azobenzene-containing Random Copolymer. *Macromolecules*, **2006**, 39, 1108–1115.
- (17)Deng, Y. H.; Li, Y. B.; Wang, X. G. Colloidal Sphere Formation, H-aggregation, and Photoresponsive Properties of an Amphiphilic Random Copolymer Bearing Branched Azo Side Chains. *Macromolecules*, **2006**, 39, 6590–6598.
- (18)Wang, Y. P.; Han, P.; Xu, H. P.; Wang, Z. Q.; Zhang, X.; Kabanov, A. V. Photocontrolled Self-assembly and Disassembly of Block Ionomer Complex Vesicles: A Facile Approach toward Supramolecular Polymer Nanocontainers. *Langmuir*, **2010**, 26, 709–715.

- (19)Bédard, M.; Skirtach, A. G.; Sukhorukov, G. B. Optically Driven Encapsulation using Novel Polymeric Hollow Shells Containing an Azobenzene Polymer. *Macromol. Rapid Commun*, **2007**, 28, 1517–1721.
- (20)Graisuwan, W.; Zhao, H.; Kiatkamjornwong, S.; Theato, P.; Hoven, V. P. Formation of Thermo-sensitive and Cross-linkable Micelles by Self-assembly of Poly(pentafluorophenyl acrylate)-containing Block Copolymer. *J. Polym. Sci. Pol. Chem.*, **2015**, 53, 1103–1113.
- (21)Feng, Z.; Lin, L.; Yan, Z.; Yu, Y. Dual Responsive Block Copolymer Micelles Functionalized by NIPAM and Azobenzene. *Macromol. Rapid Commun*, **2010**, 31, 640–644.
- (22)Karen, K.; Sukhorukov, G. B.; Heat Treatment of Polyelectrolyte Multilayer Capsules: A Versatile Method for Encapsulation. *Adv. Funct. Mater*, **2007**, 17, 2053–2061.
- (23)Yi, Q. Y.; Wen, D. S.; Sukhorukov, G. B. UV-cross-linkable Multilayer Microcapsules Made of Weak Polyelectrolytes. *Langmuir*, **2012**, 28, 10822–10829.
- (24)Wang, X. T.; Yang, Y. K.; Liao, Y. G.; Yang, Z. F.; Jiang, M.; Xie, X. L. Robust Polyazobenzene Microcapsules with Photoresponsive Pore Channels and Tunable Release Profiles. *Eur. Polym. J.*, **2012**, 48, 41–48.
- (25)Wang, X. T.; Li, Z. H.; Yang, Y. K.; Gong, X. H.; Liao, Y. G.; Xie, X. L. Photomechanically Controlled Encapsulation and Release from pH Responsive and Photoresponsive Microcapsules. *Langmuir*, **2015**, 31, 5456–5463.

- (26) Li, A. H.; Liu, J. Q.; Liu, G. Z.; Zhang, J. Z.; Feng, S. Y. Design and Synthesis of Fluorescent Core-shell Nanoparticles with Tunable Lower Critical Solution Temperature Behavior and Metal-enhanced Fluorescence. *J. Polym. Sci. Pol. Chem.*, **2014**, 52, 87–95.
- (27) Men, Y. J.; Drechsler, M.; Yuan, J. Y. Brushes with a Poly(ionic liquid) Core and a Thermoresponsive Shell. *Macromol. Rapid Commun.*, **2013**, 34, 1721–1727.
- (28) Luo, L.; Zhang, H. S.; Liu, Y.; Ha, W.; Li, L. H.; Gong, X. L.; Li, B. J.; Zhang, S. Preparation of Thermosensitive Polymer Magnetic Particles and their Application in Protein Separations. *J. Colloid Interf. Sci.*, **2014**, 435, 99–104.
- (29) Zhang, K.; Wu, W.; Guo, K.; Chen, J. F.; Zhang, P. Y. Synthesis of Temperature-Responsive Poly(N-isopropyl acrylamide) / Poly(methyl methacrylate) / Silica Hybrid Capsules from Inverse Pickering Emulsion Polymerization and their Application in Controlled Drug Release. *Langmuir*, **2010**, 26, 7971–7980.
- (30) Liu, Z. L.; Han, H.; Zhuo, R. X. Konjacglu Comannan-graft-acrylic Acid Hydrogels containing Azo Crosslinker for Colon-specific Delivery. *J. Polym. Sci. Pol. Chem.*, 2004, 42, 4370–4378.
- (31) Bai, F.; Yang, X. L.; Huang, W. Q. Synthesis of Narrow or Monodisperse Poly(divinylbenzene) Microspheres by Distillation-precipitation Polymerization. *Macromolecules*, **2004**, 37, 9746–9752.
- (32) Li, G. L.; Lei, C. L.; Wang, C. H.; Neoh, K. G.; Kang, E. T.; Yang, X. L. Narrowly Dispersed Double-walled Concentric Hollow Polymeric Microspheres with Independent pH and Temperature Sensitivity. *Macromolecules*, **2008**, 41, 9487–9490.

- (33) Mu, B.; Liu, P.; Li, X. R.; Du, P. C.; Dong, Y.; Wang, Y. J. Fabrication of Flocculation-resistant pH/Ionic Strength/Temperature Multiresponsive Hollow Microspheres and their Controlled Release. *Mol. Pharmaceutics*, **2012**, 9, 91–101.
- (34) Nayak, S.; Bhattacharjee, S.; Chaudhary, Y. S. In Situ Encapsulation and Release Kinetics of pH and Temperature Responsive Nanogels. *J. Phys. Chem. C*, **2012**, 116, 30–36
- (35) Cao, Z. Q.; Zhou, X. T.; Wang, G. J. Selective Release of Hydrophobic and Hydrophilic Cargos from Multi-stimuli-responsive Nanogels. *ACS Appl. Mater. Interfaces*, **2016**, 8, 28888–28896
- (36) Zhang, Y. Y.; Ma, Y.; Sun, J. Q. Reversible Actuation of Polyelectrolyte Films: Expansion-induced Mechanical Force enables Cis-trans Isomerization of Azobenzenes. *Langmuir*, **2013**, 29, 14919–14925.
- (37) Li, M. H.; Keller, P.; Li, B.; Wang, X.; Brunet, M. Light-driven Side-on Nematic Elastomer Actuators. *Adv. Mater.*, **2003**, 15, 569–572.
- (38) Erandimala, U.; Kulawardana; Douglas, C.; Neckers. Photoresponsive Oil Sorber. *J. Polym. Sci. Pol. Chem.*, **2010**, 48, 55–62.
- (39) Chen, T. Y.; Hu, S. H.; Liu, D. M. Biomedical Nanoparticle Carriers with Combined Thermal and Magnetic Responses. *Nano Today*, **2009**, 4, 52–65.
- (40) Köhler, K.; Shchukin, D. G.; Möhwald, H.; Sukhorukov, G. B. Thermal Behavior of Polyelectrolyte Multilayer Microcapsules. 1. The Effect of Odd and Even Layer Number. *J. Phys. Chem. B*, **2005**, 109, 18250–18259.

- (41) Higuchi, T. Mechanism of Sustained-action Medication. Theoretical Analysis of Rate of Solid Drugs Dispersed in Solid Matrices. *J. Pharm. Sci.*, **1963**, 32, 1145–1149.
- (42) Baker, R. W.; Lonsdale, H. K. Controlled Release: Mechanisms and Rates. In *Controlled Release of Biologically Active Agents*; Tanquary, A. C.; Lacey, R. E.; *Eds.* Plenum Press: New York, **1974**, 15–71.
- (43) Hu, H. R.; Wang, H. T.; Du, Q. G. Preparation of pH-sensitive Polyacrylic Acid Hollow Microspheres and their Release Properties. *Soft Matter*, **2012**, 8, 6816–6822.
- (44) Kim, J. O.; Kabanov, A. V.; Bronich, T. K. Polymer Micelles with Cross-linked Polyanion Core for Delivery of a Cationic Drug Doxorubicin. *J. Controlled Release*, **2009**, 138, 197–204.
- (45) Radin, S.; Chen, T.; Ducheyne, P. The Controlled Release of Drugs from Emulsified, Sol Gel Processed Silica Microspheres. *Biomaterials*, **2009**, 30, 850–858.